STRUCTURAL AND ELECTRICAL STUDY OF GREEN SYNTHESIZED ZINC OXIDE NANOPARTICLES USING ALOE-VERA GEL

Ravikant Divakar, Bijendra Singh, Ashish Bajpai, Sunder Singh And Anil Kumar
Department of Physics, Hindu College, Moradabad
Affiliated to Mahatma Jyotiba Phule Rohilkhand University, Bareilly, U.P. (INDIA)
Email: ravikant@hinducollege.edu.in

Abstract

The zinc oxide nanoparticles are prepared by green synthesis method using aloe-vera gel. The prepared nanoparticles are calcined at 500°C. The crystallite size is determined from the XRD analysis using Scherrer's formula. The X-rays diffraction (XRD) analysis indicates the hexagonal crystal structure of zinc oxide. The hexagonal crystal structure is confirmed with help of Rietveld refinement of the XRD of the sintered zinc oxide. The electrical behavior of zinc oxide is studied using impedance spectroscopy. It is found that the ac conductivity of zinc oxide is frequency and composition dependent. The activation energy is calculated at high and low temperature respectively.

Keywords*: Aloe-vera, green synthesis, impedance, nanoparticles, Rietveld refinement, zinc oxide,*

1. Introduction

In the past decade, tremendous increase interest in the nanotechnology due to their exceptional properties such as greater surface area, quantum confinement effect, good catalytic activity, etc. Nanoparticles are very small sized particles range from 10nm-100nm with enhanced chemical activity, thermal conductivity and non-linear optical performance with reference of their large surface area to volume ratio [1]. Nanoparticle are synthesized physical and chemical methods. The special equipment and skilled labor are required for synthesis of nanoparticles using many chemical, and physical methods such as hydrothermal, laser ablation, lithography, etc. Moreover, these methods are unsafe to human health due to toxic effect [2-3]. The green synthesis of nanoparticles is found to be cost-effective, non-toxic, and ecofriendly approach [4]. The ecofriendly synthesis approach reduces the use of toxic chemical. In this method, the natural extract of leaves, stems, roots, flower, and seeds etc. Plant parts such as roots, leaves, seeds, stems, fruits are used for the nanoparticles synthesis because their extract is rich in phytochemicals which acts as reducing and stabilization agent both [5]. Green synthesized metal oxide nanoparticles are free from toxic effect of chemicals and additional impurities.

The semiconducting nanostructures with wide band gap such as zinc oxide (ZnO), indium oxide (In_2O_3), tin oxide (SnO_2) and doped oxide are extensively studied in recent years [6-8]. Zinc oxide has attracted great interest of researchers due to its optical, piezoelectric, magnetic, gas sensing and electrical properties. Zinc oxide have tremendous semiconducting properties (II-VI) due to its wide band gap (3.37eV) and high exciton binding energy (60meV) at room temperature [9]. Study of physical properties like electrical conductivity of zinc oxide can be done by impedance spectroscopy [10]. It has also described in the literature that the zinc oxide nanostructures can studied by Rietveld refinement.

The electrical properties of green synthesized zinc oxide nanoparticle are very less studied. The electrical properties altered by additive dopant due to extrinsic defects in pure zinc oxide [11].

In present study we have investigated the structural properties using Rietveld refinement and the electrical properties such as ac conductivity, and impedance of zinc oxide using impedance spectroscopy.

2. Materials and Method

2.1 Materials

Fresh leaves of aloe-vera plant were collected from Buddhi Vihar, Moradabad, Uttar Pradesh. The chemicals zinc nitrate hexahydrate ($Zn(NO_3)_2.6H_2O$), and cupric nitrate hexahydrate ($Cu(NO_3)_2.6H_2O$) were purchased from M.S. Scientific.

2.2 Preparation of extract

The collected leaves of aloe-vera were cleaned under the running tape water to eliminate the impurities. Later, the aloe-vera leaves were cleaned using distilled water. Then, the leaves were dried in a dark room. The gel of aloe-vera was extracted from the leaves using stainless steel knife. Later, prepared aloe-vera gel was filtered using a filter of pore size 0.1 mm made of stainless steel to remove excess residual. The fresh of aloe-vera gel was used in further synthesis process as shown in fig. 1. The aloe-vera gel was used as capping or stabilizing during the synthesis process of nanoparticles.

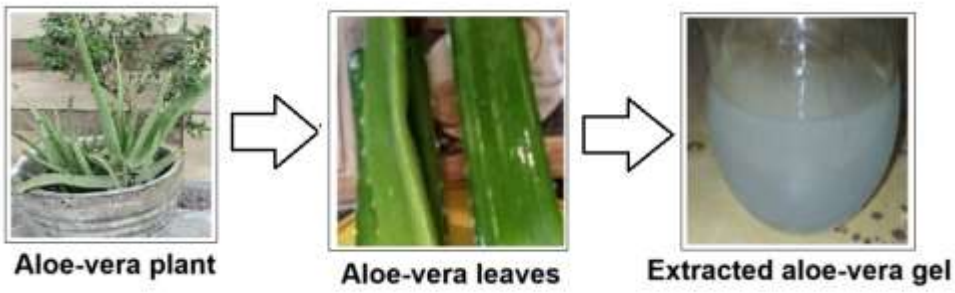

Fig. 1 Procedure for extraction of aloe-vera gel from the leaves of aloe-vera plant

2.3 Green synthesis of nanoparticles

The current research work was done at Department of Physics, Hindu College Moradabad. The solution of the zinc nitrate hexahydrate of 0.1 molarity was prepared using distilled water. Subsequently, 20ml of aloe-vera gel was added slowly in the 100ml solution of prepared zinc nitrate under vigorous stirring using magnetic stirrer at room temperature to get a homogeneous solution. Initially, the colour of prepared solution was light milky. This solution was stirred at 55-65^{o}C for an hour and put it overnight to complete the reaction. The solution was dried under stirring at 75^{o}C until the solution turns to dark brown gel. The change in colour of the solution is a visual indication of formation of the nanoparticles. This gel like solution was calcined at 500^{o}C in hot air oven for an hour. The sample was crushed using mortar-pestle for 15min to obtain final product in fine powder form as shown in fig. 2. The prepared sample was stored for further characterization.

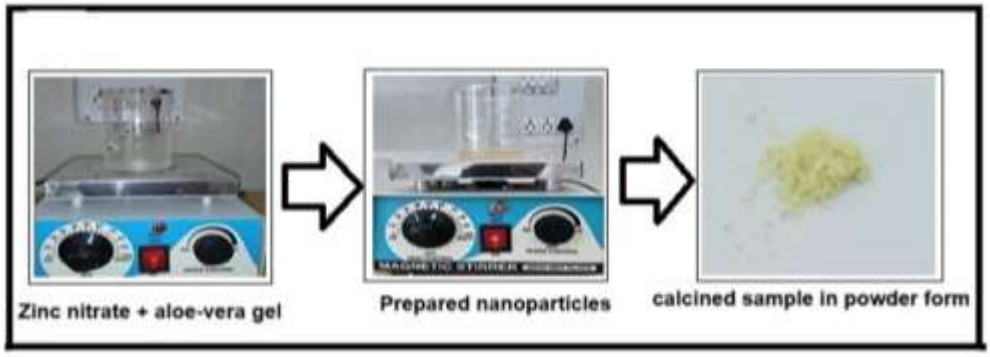

Fig. 2 Procedure of green synthesis of zinc oxide nanoparticle using aloe-vera gel

2.4 Preparation of Pellet:

The polyvinyl alcohol (PVA) was added to the distilled water in the ratio of 1:25. The magnetic stirrer with hot plate was used to boil it under vigorous stirring to get dissolved in water. The PVA solution was used as binder. Some drops were sprinkled on 0.4gm of prepared nanoparticles. The sample was then mixed by mortar and pestle to get it dried. The sample was placed in hydraulic press machine and applied 2 tons pressure for 2 min. The fine pellet of prepared sample was obtained. Furthermore, the cool sintering of the prepared pallet was undertaken in hot air oven at 450^{o}C for 60min. The pellet was stored for further analysis.

3. Results and Discussion

3.1 Structural properties

The structural properties of as prepared zinc oxide nanoparticles are determined with help of following analysis: -

3.1.1 X-ray diffraction analysis

The X-ray diffraction (XRD) patterns of green synthesized sample calcined at 500^{o}C and pallet sintered at 450^{o}C are shown in fig.3. It was observed that no extra peak of impurity was present in the XRD pattern. It was observed single phase in prepared sample. The XRD spectra define the wurtzite hexagonal structure with P 63 mc space group symmetry of zinc oxide which was confirmed from the JCPDS card No. 00-036-1451. It is observed that the green synthesized ZnO nanoparticles are free from impurity.

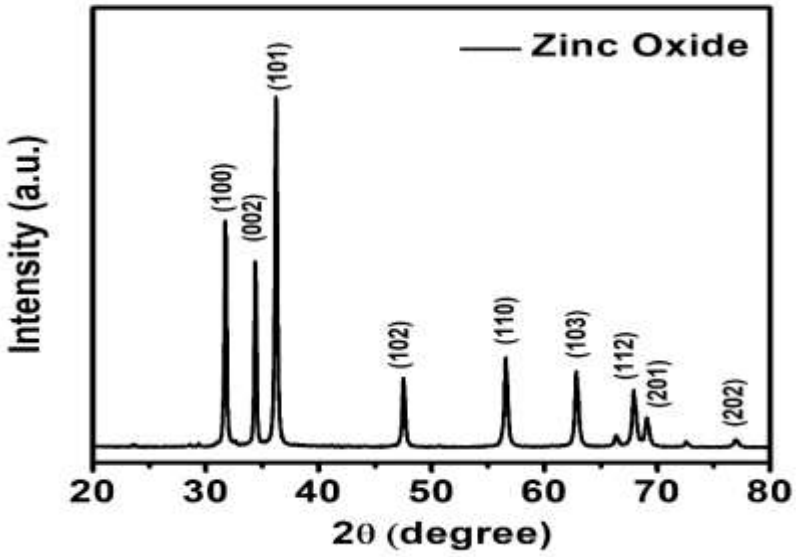

Fig. 3 XRD pattern of zinc oxide pellet sintered at 450°C temperature

The crystallite size was determined using Scherrer's formula [12],

$$D = \frac{0.9\lambda}{\beta \cos\theta} \quad (1)$$

Where λ is wavelength of X-ray radiation, β defines the full width at half maxima (FWHM) of the observed peaks at diffracting angle 2θ. The crystallite size of zinc oxide is calculated using Scherrer formula given in eq. (1). The average crystallite size of zinc oxide nanoparticles is found 39.8 nm.

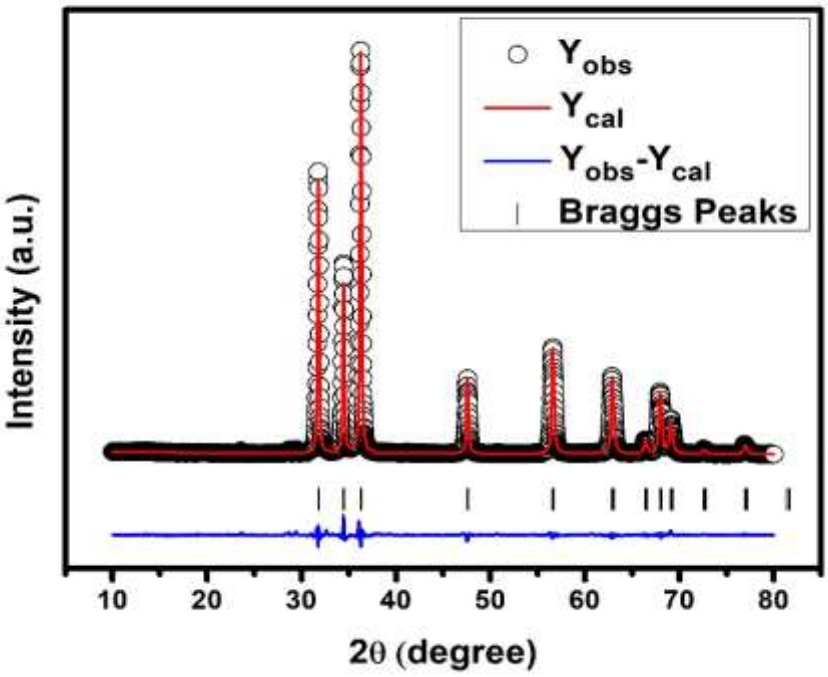

Fig. 4 Rietveld refinement of XRD pattern of sintered pellet at 450°C temperature of zinc oxide.

The wurtzite hexagonal structure with P 63 mc space group symmetry of zinc oxide was detected in the XRD pattern by Rietveld refinement using FullProof software of sintered pellet at 450°C as shown in fig. 4 [13]. The refined structural parameters are represented in Table 1.

Table 1 Refined structural parameters via Rietveld refinement of zinc oxide sintered at 450°C

T (°C)	Lattice parameter (Å)	Volume (Å^3)	Rietveld refined parameters	Bond Length (Å) [Zn1-O1]
450	a = b = 3.2493, c = 5.2057	47.60	R_p = 9.11, R_{wp} = 10.9, R_{exp} = 7.25, χ^2 = 2.27	1.98

3.1.2 FESEM analysis

FESEM image of prepared nanostructured sample is shown in fig. 6. It is observed the agglomerated form of nanoparticles which is confirmed by the surface morphology. The effect of surface morphology and its connection in synergistic activity of ZnO [14]. The average grain size is calculated using imageJ software. The average grain size of zinc oxide is found 41.33 nm.

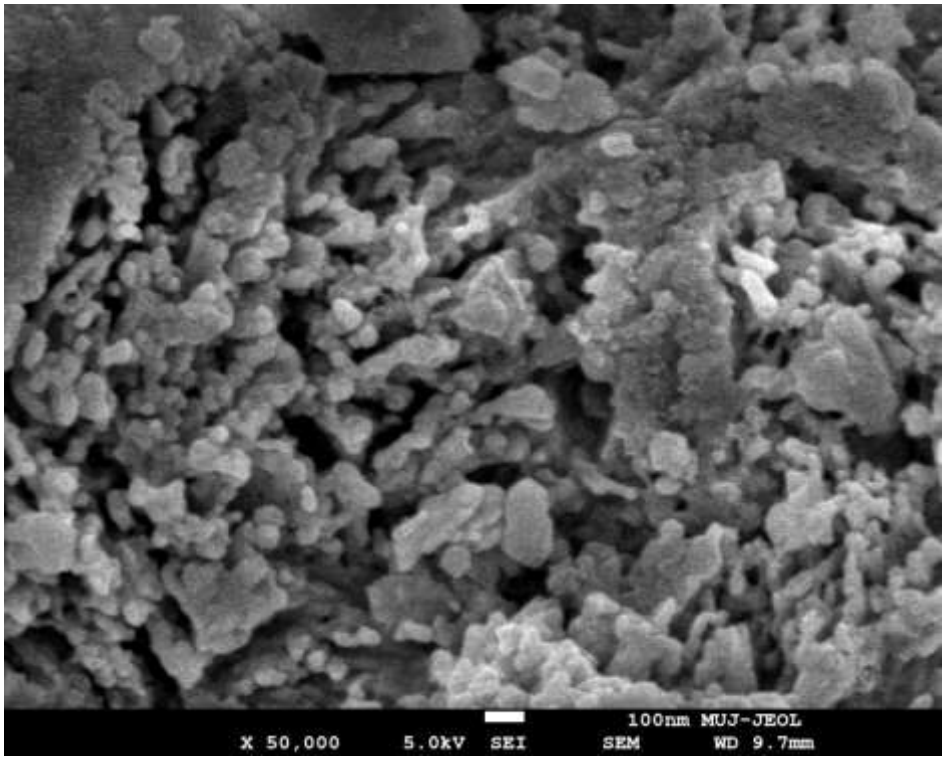

Fig. 6 FESEM image of zinc oxide nanoparticles calcined at 500ºC

3.1.3 EDX Analysis

EDX patterns in fig. 7 are exposed strong signal for zinc and oxygen, which confirms the presence of zinc in the oxide form. The composition of each element is obtained from EDX analysis data. The obtained atomic and weight are 35.1%, and 68.9% of zinc respectively, and 64.9% and 31.1% of oxygen respectively zinc oxide. Two sharp peaks were observed for zinc at 1.1eV and 8.7eV, the signal for oxygen was observed at 0.6eV. These values are dissimilar for zinc and oxygen, which establishes the elemental composition of the synthesized compound (ZnO).

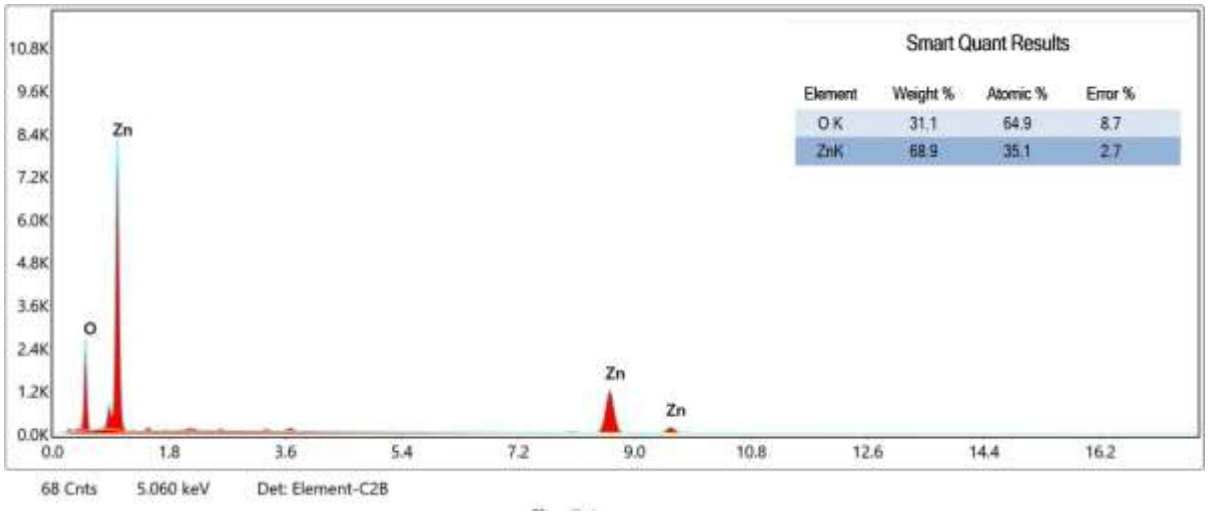

Fig. 7 EDX spectrum of zinc oxide nanoparticles

3.2 Electrical Properties

3.2.1 AC conductivity

The fig. 8 represents the variation in ac conductivity at different temperatures for zinc oxide and was calculated by the formula $\sigma_{ac} = Z'd/[(Z')^2 + (Z'')^2]A$, where A and d are the area and thickness of the sample. Furthermore, the variation in σ_{ac} with frequency is represented in fitted curve fig. 8 for zinc oxide using Jonsher's universal power law as given in eq. (2). It reveals the typical behaviour of semiconducting materials: the conductivity is found to be frequency dependent at low temperature and frequency independent at higher temperature in low frequency (dc plateau) for zinc oxide. The range and magnitude of ac conductivity plateau towards the lower frequency region is increased, as shown in fig. 8 for zinc oxide.

The universal power law proposed by Jonscher is used to fit frequency dependent ac conductivity spectra given as

$$\sigma_{ac} = \sigma_{dc}\left[1 + \left(\frac{f}{f_H}\right)^n\right] \quad (2)$$

Here, σ_{ac} is the total conductivity, f_H is hopping frequency of charge carriers, σ_{dc} represent dc conductivity, and n ($0 < n < 1$) is frequency exponent and interpret interaction between charge carriers and lattice. The term $\sigma_{dc}\left(\frac{f}{f_H}\right)^n$ defines the conduction properties of charge carriers (electrons, holes, ions, and polarons) in polycrystalline materials. The ac conductivity data is best fitted by the universal power law, and fitting parameters are presented in Table 1. However, the deviation in the value of frequency exponent (n) is defined range of 0-1 and found to be between 0.2502 and 0.5002 for zinc oxide.

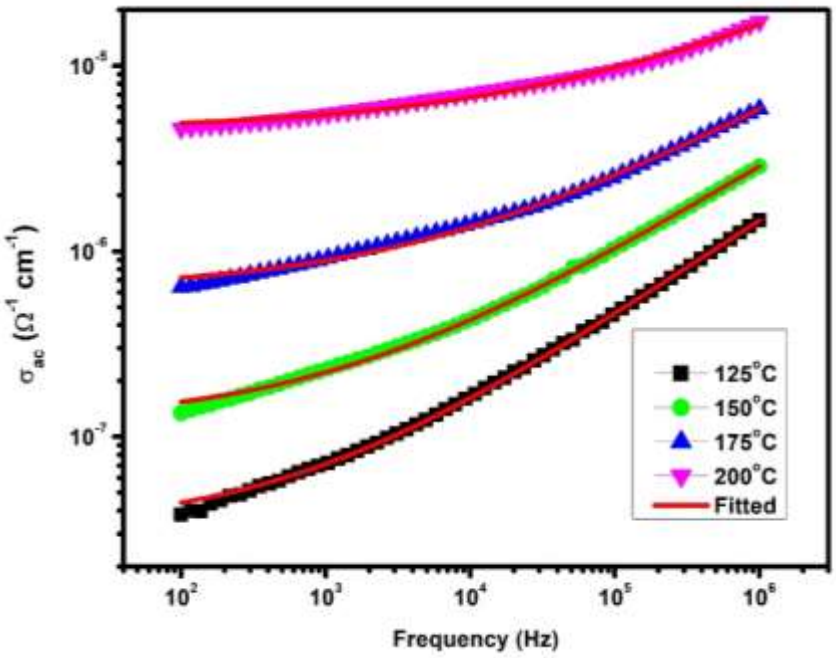

Fig. 8 Frequency dependence of ac conductivity zinc oxide at various temperatures

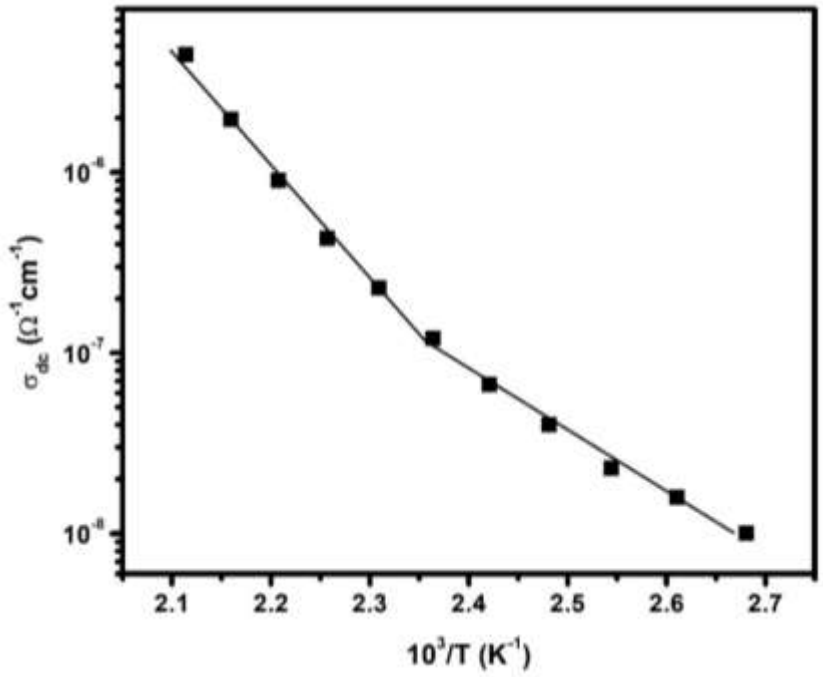

Fig. 9 The variation of ac conductivity with temperature of zinc oxide

The temperature dependent dc conductivity in accordance with the Arrhenius relation is given by

$$\sigma_{dc} = \sigma_0 \exp\left(-\frac{E_a}{k_B.T}\right) \quad (3)$$

Where, σ_0 is constant (pre-exponential factor), and E_a defines the activation energy related with this conduction process, k_B is the Boltzmann constant and T is the temperature.

Two linear sections in the graph between 1000/T and log of dc conductivity (σ_{dc}) are shown in fig. 9 which slope represents the value of activation energy (E_a) of charge carriers of ZnO. The values of E_a have been obtained from the slope of straight line. The calculated values of activation energy are $E_{a(1)}$= 0.592 eV, and $E_{a(2)}$= 0.310 eV at high and low temperature respectively as shown in fig. 9.

Table 2 The fitting parameters of ac conductivity with Jonsher's law for pure zinc oxide

T (°C)	σ_{dc} ($\Omega^{-1}cm^{-1}$)	a	n
120	2.0634×10^{-8}	1.5311×10^{-9}	0.5002
130	4.1673×10^{-8}	2.5808×10^{-9}	0.4872
140	7.3847×10^{-8}	4.7640×10^{-9}	0.4661
150	1.3929×10^{-7}	8.5051×10^{-9}	0.4479
160	2.4964×10^{-7}	1.7829×10^{-8}	0.4175
170	4.3109×10^{-7}	3.9139×10^{-8}	0.3820
180	7.8073×10^{-7}	8.5883×10^{-8}	0.3496
190	1.4438×10^{-6}	2.4124×10^{-7}	0.3046
200	2.5318×10^{-6}	9.5965×10^{-7}	0.2502

3.2.2 Impedance Analysis

The fitting of the experimental data using eq. 4 is denoted by a solid line in Fig. 10 zinc oxide at various temperatures. It is observed that at each temperature, the values of $(-Z'')$ shifted to higher frequency when temperature rises zinc oxide and increases in lower frequency region reaches to a maximum value. This is a suggestion of the temperature dependency of relaxation time in such polycrystalline sample. The electrical process arises in material is stimulated using an equivalent circuit as shown in fig. 13. The experimental impedance data is fitted by the Z-Simpwin software using an electrical circuit defined in fig. 10 for zinc oxide.

Therefore, the cole-cole function may be used to define the three contribution effects in impedance data [15] as given in equation (4),

$$Z^* = \frac{R_g}{(1+j\omega R_g C_g)^{ag}} + \frac{R_{gb}}{(1+j\omega R_{gb} C_{gb})^{agb}} + \frac{R_g}{(1+j\omega R_e C_e)^{\alpha e}} \quad (4)$$

Where R_g, R_{gb}, and R_e are the resistance related to grain, grain boundary, and electrode respectively and C_g, C_{gb}, and C_e are capacitance of the grain, grain boundary and electrode respectively while α is associated with distribution of time of realaxation which leads to the broadening of Debye relaxation peak, lies between 0 and 1.

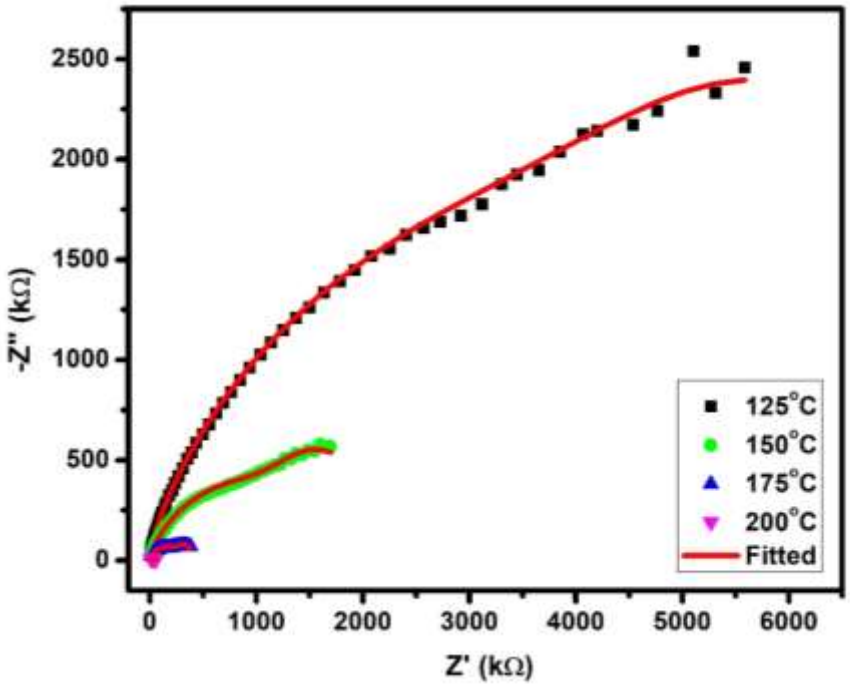

Fig. 10 Variation in imaginary part of impedance $(-Z'')$ with real part of impedance (Z') at various temperature zinc oxide

The variation in frequency-dependent real part of impedance (Z') is shown in fig. 11 at various temperatures. The fitting of experimental data using real part of impedance (Z') of eq. 4 is denoted by a solid line as shown in fig. 11. It is observed that Z' is associated with resistance of zinc oxide which declines with growing temperature and frequency. This behaviour indicate increment in the electrical conduction of charge carrier for higher temperature and frequency for zinc oxide as shown in fig. 11. The dispersion curve appears to be merged at higher frequency region, indicating possible release of space charge due to depletion of potential barrier.

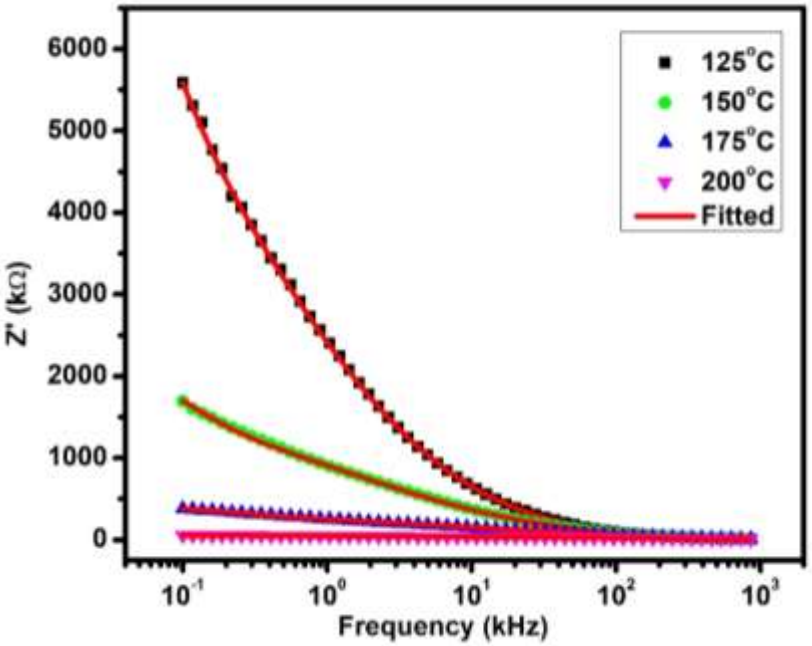

Fig. 11 Variation in real part of impedance (Z′) with frequency at various temperature for zinc oxide

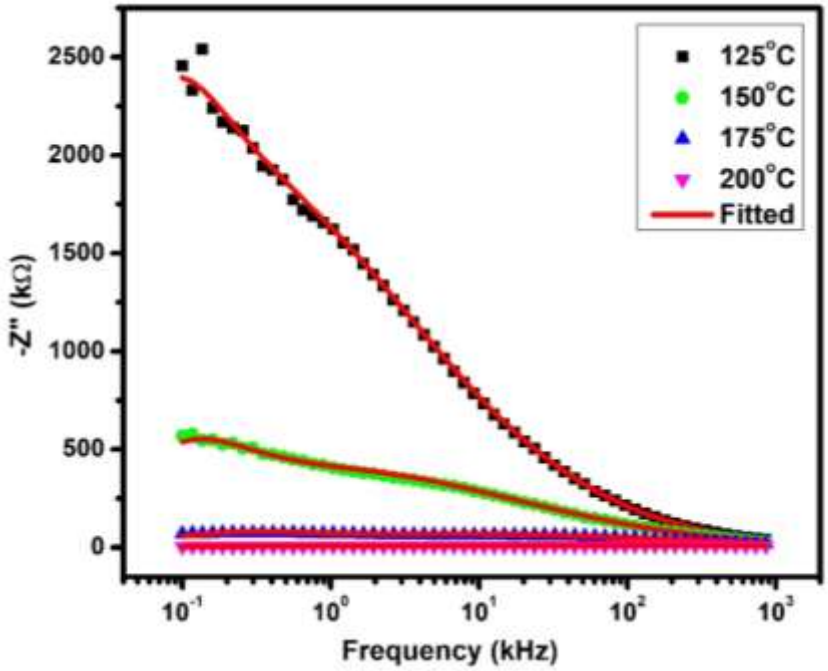

Fig. 12 Variation in imaginary part of impedance (−Z") with frequency at various temperature for zinc oxide

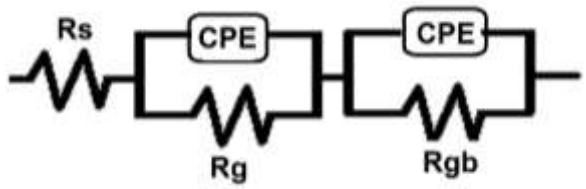

Fig. 13 Electrical equivalent circuit used to fit the Nyquist plots

The frequency dependent imaginary part of impedance $(-Z'')$ at various temperature shown in fig. 12. The experimental data is fitted using imaginary part of impedance $(-Z'')$ of eq. (4) represented by a solid line in zinc oxide respectively. It is clearly in plots mentioned below that considerable change in the shape and nature of plot at various temperatures and frequencies. Consequently, plot of imaginary part of impedance $(-Z'')$ seems to merged at higher frequency region. This property of curve is mainly due presence of space charge polarisation process, which is inconsiderable at high frequencies.

4. Conclusion

The study provides an eco-friendly, cost effective and simple approach for the synthesis of zinc oxide nanoparticles using aloe-vera gel. The plant extract contains several phytochemicals act as both reducing, and capping or stabilizing agent. In present study, zinc oxide nanoparticles were synthesized using aloe-vera gel. The prepared sample was calcined at 500°C. The XRD analysis also confirms the hexagonal (wurtzite) crystal structure of zinc oxide. The Rietveld refinement of the XRD of zinc oxide sintered at 450°C confirmed the hexagonal structure with P 63 mc space group symmetry. The average crystallite size was calculated using Scherrer's and found 39.8 nm zinc oxide. The FESEM images and EDX analysis confirmed the presence of zinc in oxide form. The electrical behavior of zinc oxide was studied using impedance spectroscopy. It was found that the ac conductivity is frequency and composition dependent. The calculated values of activation energy are $E_{a(1)}$= 0.592 eV, and $E_{a(2)}$= 0.310 eV at high and low temperature respectively.

References

[1] S. T. Khan, J. Mussarat, and A. A. Al-Khedhairy, Countering drug resistance, infectious diseases, and sepsis using metal and metal oxide nanoparticles, Colloids and Surface B: Biointerfaces, Vol. 146, pp. 70-83, 2016.

[2] J. Virkutyte, R.S. Varma, Green synthesis of metal nanoparticals: biodegradable polymer and enzymes in stabilization and surface functionalization, Chem. Sci., Vol. 2, pp. 837-846, 2011.

[3] M. Darroudi, Z. Sabouri, R.K. Oskuee, A.K. Zak, H. Kargar, M.H.N.A. Hamid, Green chemistry approach for the synthesis of ZnO nanopowders and their cytotoxic effects, Ceram. Int., Vol. 40, pp. 4827-4831, 2014.

[4] D. Jain, H.K. Daima, S. Kachhwaha, S.L. Khothari, Synthesis of plant-mediated silver nanoparticles using papaya fruit extract and evaluation of their antimicrobial activities", Digest Journal of Nanomaterials and Biostructures, Vol. 4, pp. 557-563, 2009.

[5] P. Mukherjee, M. Roy and B. Mandal., Green synthesis of highly stabilized nanocrystalline silver nanoparticles silver particles by non-pathogenic and agriculturally important fungus T. asperellum, Nanotechnology, Vol. 19, pp. 75103-75110, 2008.

[6] Apurva Dev, S. Chaudhuri, B.N. Dev, Bull. Mater. Sci., Vol. 31, pp. 551-559, 2008

[7] A.S. Ahmed, A. Azam, M. Shafeeq, M. Chaman, T. Tabassum, J. Phys. Chem. Solids, Vol.73, pp. 943-947, 2012.

[8] B.U. Haq, A. Afaq, R. Ahmed, S. Naseem, Chanese Phys. B, Vol. 12, pp. 97-101, 2012.

[9] T.N. Soitah, Y. Chunhui, S. Liang, Sci. Adv. Mater, Vol. 2, pp. 534-538, 2010.

[10] X.S. Wang, Z.C. Wu, J.F. Webb, Z.G. Liu, Appl. Phys. A: Mater. Sci. Process, Vol. 77, pp. 561-565, 2003.

[11] H. Abdullah, M.N. Nozarzia, S. Shaari, M.Z. Nuawi, N.S. Mohamed Dan, Am. J. Eng. Appl. Sci., Vol. 3, pp. 171-179, 2010

[12] A.L. Patterson, The Scherrer formula for X-ray particle size determination, Phys. Rev. Online Arch. (Prola), Vol. 56, pp. 978-982, 1939.

[13] H.E. Okur, N. Bulut, T. Ates, and O. Kaygili, Structural and optical characterization of Sm-doped ZnO nanoparticles, Bull. Mater. Sci., Vol. 42(199), pp. 1-9, 2019.

[14] X. Peng, S. Palma, N.S. Fisher, S.S. Wong, Effect of morphology of ZnO nanostructures on their toxicity to marine algae, Aquat. Toxicol., Vol. 102, pp. 186–196, 2011.

[15] Deepash Shekhar Saini, Shuvendu Tripathy, Aparabal Kumar, Sanjeev Kumar Sharma, Avijit Ghosh, Debasis Bhattacharya, Impedance and modulus spectroscopic analysis of single phase BaZrO3 ceramics for SOFC application, Ionics, Vol. 24, pp. 1161–1171, 2018.